HHS Public Access

Author manuscript

Genes Immun. Author manuscript; available in PMC 2014 March 01.

Published in final edited form as:

Genes Immun. 2013 September ; 14(6): 373–379. doi:10.1038/gene.2013.28.

The combination of two *Sle2* lupus-susceptibility loci and *Cdkn2c* deficiency leads to T cell-mediated pathology in B6.*Fas*^{lpr} mice

Zhiwei Xu[1], **Byron P. Croker**[1,2], and **Laurence Morel**[1]

[1]Department of Pathology, Immunology, and Laboratory Medicine, University of Florida, Gainesville, FL 32610

[2]North Florida South George Veterans Health System, Gainesville, FL 32608

Abstract

The NZM2410 *Sle2c1* lupus susceptibility locus is responsible for the expansion of the B1a cell compartment and for the induction of T-cell induced renal and skin pathology on a CD95 deficient (Fas^{lpr})-background. We have previously shown that deficiency in cyclin-dependent kinase inhibitor p18^{INK4c} (p18) was responsible for the B1a cell expansion but was not sufficient to account for the pathology in B6.lpr mice. This study was designed to map the additional *Sle2c1* loci responsible for autoimmune pathology when co-expressed with CD95 deficiency. The production, fine-mapping and phenotypic characterization of five recombinant intervals indicated that three interacting sub-loci were responsive for inducting autoimmune pathogenesis in B6.*lpr* mice. One of these sub-loci corresponds most likely to p18-deficiency. Another major locus mapping to a 2 Mb region at the telomeric end of *Sle2c1* is necessary to both renal and skin pathology. Finally, a third locus centromeric to p18 enhances the severity of lupus nephritis. These results provide new insights into the genetic interactions leading to SLE disease presentation, and represent a major step towards the identification of novel susceptibility genes involved in T-cell mediated organ damage.

Keywords

Systemic Lupus Erythematosus; congenic dissection; epistatic interaction; T cells; CD95

INTRODUCTION

Systemic lupus erythematosus (SLE) is a prototypic autoimmune disease characterized by production of autoantibodies (autoAb)including dsDNA and chromatin, followed by inflammation and damage in multiple organs, such as the kidneys and the skin.[1] In spite of

Correspondence: Zhiwei Xu or Laurence Morel, Department of Pathology, Immunology and Laboratory Medicine, University of Florida, Gainesville, FL 32610-0275, USA. Tel: (352) 392-3790, Fax: (352) 392-3053. morel@ufl.edu.

Disclosures

The authors have no financial conflict of interest.

striking advances in the last few years, the identification of lupus-susceptibility genes and their causative variants still constitutes a great challenge, although it represents a critical step to fully understand SLE pathogenesis.[2] Murine models have led to the discovery of a large number of genomic intervals associated with lupus susceptibility or SLE-related phenotypes.[3] Only a few murine candidate genes have been proposed with a reasonable degree of confidence for causative etiology, and they have been implicated either in immune tolerance, autoimmune amplification or end-organ damage.[3]

We have identified by linkage analysis three susceptibility loci, *Sle1*, *Sle2* and *Sle3*, that collectively represent the genomic variants that are necessary and sufficient for lupus-prone NZM2410 mice to develop clinical disease.[4, 5] The autoimmune phenotypes resulting from *Sle2* expression on a C57BL/6 (B6) background have been largely linked to B cells.[6–9] A congenic dissection of the *Sle2* locus based on the expansion of the peritoneal B1a cell compartment has identified three sub-loci, *Sle2a*, *Sle2b* and *Sle2c*.[10] *Sle2a* and *Sle2b*, but not *Sle2c* mediated autoimmune disease in combination with the *Sle1* and *Sle3* loci.[10] We have further shown that the lack of contribution of *Sle2c* to autoimmune pathogenesis was due to the presence of a suppressive locus at the telomeric end of *Sle2c*, termed *Sle2c2*.[11] The centromeric portion of *Sle2c*, *Sle2c1*, is the strongest contributor to B1a cell expansion.[12] Within the *Sle2c1* interval, a polymorphism in the promoter of the *Cdkn2c* gene results in a 5-fold decreased expression of the cyclin dependent kinase inhibitor $P18^{INK4c}$ (p18).[13] By comparing the phenotypes of B6.*Sle2c1* to that of B6.$p18^{-/-}$ mice, we have shown that p18 deficiency is the principal cause of B1a cell expansion.[14] The *Sle2c1* phenotypes are however not limited to B1a cells. Recently, we have bred CD95 deficiency (Fas^{lpr} allele) onto *Sle2c1* to characterize its contribution to SLE pathogenesis using a similar strategy as described for *Sle1*.[15] We found that by 4–6 months of age, *Sle2c1.lpr* mice showed a significantly enhanced lymphadenopathy as compared to B6.*lpr*, and developed dermatitis and T-cell mediated glomerulonephritis (GN), a fully novel phenotype for the *Sle2 l*ocus.

The analysis of B6.$p18^{-/-}$.*lpr* mice revealed that p18-deficiency contributed only partially to the autoimmune pathogenesis in *Sle2c1.lpr* mice.[14] The present study was designed to map which additional loci within *Sle2c1* interacted with CD95 deficiency to produce autoimmune pathogenesis. We have produced and fine-mapped five new strains combining CD95 deficiency with *Sle2c1* recombinant intervals. A comprehensive phenotypic analysis of these congenic strains indicated that three interacting sub-loci were responsive for inducting autoimmune pathogenesis in B6.*lpr* mice. One of these sub-loci corresponds most likely to p18-deficiency. Another major locus mapping to a 2 Mb region at the telomeric end of *Sle2c1* is necessary to both renal and skin pathology. Finally, a third locus centromeric to p18 enhances the severity of lupus nephritis. These results provide new insights into the genetic interactions leading to SLE disease presentation, and represent a major step towards the identification of novel susceptibility genes involved in T-cell mediated organ damage.

RESULTS

Production and fine-mapping of Sle2c1.lpr recombinant strains

In order to map the phenotypes of the *Sle2c1.lpr* strain,[12] we have bred the *lpr* mutation onto three existing *Sle2c1* recombinants,[10] *Sle1c1.rec1*, *Sle1c1.rec1a* and *Sle2c1.rec1b*. In addition, we have produced two new recombinants, *Sle2c1.rec1c.lpr* and *Sle2c1.rec1d.lpr*, totaling five *Sle2c1.lpr* sub-strains (Fig. 1). The *Sle2c1* interval represents ~ 13 Mb of chromosome 4 NZB-derived genome between D4Mit119 and D4Mit11.[10] We have fine-mapped the five recombinant intervals using all the possible markers that are polymorphic between the NZB and B6 genomes, including microsatellites and single nucleotide polymorphisms (SNPs) collected from the Mouse Genome Informatics (MGI) and the National Center for Biotechnology Information (NCBI) or identified through our own genomic sequencing (Table 1). *Sle2c1.rec1* corresponds to an interval ~ 10 Mb between the rs28166289 and rs27480282 markers. *Sle2c1.rec1b* and *Sle2c1.rec1c* correspond to non-overlapping intervals at the proximal and distal ends of *Sle2c1.rec1*, respectively. The relatively longer *Sle2c1.rec1a* and *Sle2c1.rec1d* intervals cover the *Sle2c1.rec1b* and *Sle2c1.rec1c* regions, respectively, and share a ~ 5 Mb overlap at the middle of *Sle2c1.rec1* that includes the p18 gene. We have therefore produced five overlapping recombinant intervals covering the entire *Sle2c1* locus that should allow the genetic analysis of its interaction with CD95 deficiency. The phenotypes of B6.$p18^{-/-}$.*lpr*, some of which have already been reported,[14] will also be included in the analysis to map which of the *Sle2c1.lpr* phenotypes map to the *Cdkn2c* gene itself.

Production of autoAb and lymphoid expansion

We have previously shown that *Sle2c1.lpr* but not B6.$p18^{-/-}$.*lpr* mice produced significantly more anti-dsDNA and anti-chromatin IgG than B6.*lpr* mice.[12, 14] The recombinant strains map anti-dsDNA IgG production to the *Sle2c1.rec1d* interval (Fig. 2A). Anti-chromatin IgG was significantly higher in *Sle2c1.rec1.lpr* than in B6.*lpr* mice (Fig. 2B). The difference did not reach significance for *Sle2c1.rec1d.lpr* mice although the trend was in the same direction as for anti-dsDNA. Anti-nuclear IgG production in the *rec1a*, *rec1b* and *rec1d* intervals combined to *lpr* was similar to B6.*lpr*.

Lymphoid expansion, measured as spleen and lymph node weights, was significantly higher in *Sle2c1.lpr* and B6.$p18^{-/-}$.*lpr* than in B6.*lpr* mice.[12, 14] Larger spleens and lymph nodes were found in *Sle2c1.rec1a.lpr* and *Sle2c1.rec1d.lpr* mice (Fig. 2C and D). Similar results were obtained with total splenocyte and lymph node (LN) cell numbers, and affected both B cells and $CD3^+$ T cells (data not shown). These results showed that the *rec1d* interval is involved in both anti-nuclear Ab production and lymphoid expansion while the *rec1a* interval and p18-deficiency contribute to lymphoid expansion.

Alterations in T cell subpopulations and activation

Sle2c1 preferentially expanded $CD3^+$ T cells to the expense of B cells, and this phenotype was enhanced in LNs as compared to the spleen.[12] Therefore, we examined the relative proportion of T and B cells in each recombinant interval in these two tissues. The percentage of T cells showed a significant increase in *Sle2c1.rec1a.lpr*, *Sle2c1.rec1d.lpr* and

Sle2c1.rec1.lpr spleens and LN as compared to B6.*lpr* (Fig. 3A). In addition, T cell expansion was greater in the LN than spleens of these mice, as illustrated by a 14-fold increase in the average T cell number in the *Sle2c1.rec1d.lpr* vs. B6.*lpr* LN as opposed to a 4-fold increase in the spleens from the same strains. As previously reported, the percentage of T cells in B6.*p18*$^{-/-}$.*lpr* was significantly higher than in B6.*lpr* LN but not spleens.[14] The percentage of T cells in *Sle2c1.rec1b.lpr* and *Sle2c1.rec1c.lpr* mice were similar to B6.*lpr*. The T cell expansion was mirrored by a corresponding decreased percentage of B cells in all concerned strains, including in the B6.*p18*$^{-/-}$.*lpr* spleens (Fig. 3B). These results showed that the preferential T cell expansion that we have reported in *Sle2c1.lpr* mice maps to the *Sle2c1.rec1a* and *Sle2c1.rec1d* intervals, as well as to *p18* deficiency.

T cell expansion in *Sle2c1.lpr* mice disproportionally affected CD3$^+$ CD4$^-$ CD8$^-$ T cells (double negative DN) and CD3$^+$ B220$^+$ T cells,[12], which are greatly expanded by Fas-deficiency.[16, 17] The percentage of CD3$^+$ B220$^+$ and DN T cells was significantly increased in *Sle2c1.rec1.lpr*, *Sle2c1.rec1a.lpr* and *Sle2c1.rec1d.lpr* as compared with B6.*lpr* spleens and LN (Fig. 3C and D). In addition, the percentage of DN T cells was significantly higher in *Sle2c1.rec1c.lpr* than in B6.*lpr* LN, and there was a trend for the percentage of CD3$^+$ B220$^+$ cells in the same strain (two-sided t test: p = 0.023). The percentage of DNT cells was similar in the *Sle2c1.rec1.lpr* and *Sle2c1.rec1a.lpr* spleens, but markedly lower than in *Sle2c1.rec1d.lpr* (Fig. 3D). Finally, the percentages of CD3$^+$B220$^+$ and DN T cells was similar between B6.*p18*$^{-/-}$.*lpr* and *Sle2c1.rec1a.lpr* mice, except for DN T cells, which were lower in B6.*p18*$^{-/-}$.*lpr* spleens(Fig. 3D).

The interaction between *Sle2c1* and Fas-deficiency impacted CD4$^+$ T cell functions with an increased percentage ofCD4$^+$CD44$^+$ effector T cells (Teff), and a decreased percentage of CD4$^+$FoxP3$^+$ regulatory T cells (Treg).[12] Therefore, we evaluated changes in effector T cell subsets from the LN of the five recombinant congenic mice.*Sle2c1.rec1.lpr*, *Sle2c1.rec1a.lpr* and *Sle2c1.rec1d.lpr* mice showed a significantly higher percentage of CD69$^+$ activated CD4$^+$ T cells than B6.*lpr* controls (Fig. 4A). The percentages of activated CD4$^+$ T cells was similar between *Sle2c1.rec1.lpr* and *Sle2c1.rec1a.lpr* mice, and significantly lower than in *Sle2c1rec1d.lpr* mice (Fig. 4A). Similarly, the percentage of Teff was significantly increased in *Sle2c1.rec1.lpr*, *Sle2c1.rec1a.lpr* and *Sle2c1.rec1d.lpr* mice when compared with B6.*lpr* controls (Fig. 4B). Interestingly, *Sle2c1.rec1c.lpr* mice also displayed a significantly higher percentage of Teff than B6.*lpr* mice, but it was lower than in the three other recombinant strains. In contrast, the percentage of Treg was significantly reduced and to the same extent in *Sle2c1.rec1.lpr*, *Sle2c1.rec1a.lpr*, *Sle2c1.rec1c.lpr* and *Sle2c1.rec1d.lpr* mice as compared with B6.*lpr* control. In addition, we detected a mild decrease in the percentage of Tregs in *Sle2c1.rec1b.lpr* mice as compared with B6.*lpr* (Fig. 4C). We confirmed as previously reported,[14] that the percentage of Teff was significantly higher in B6.*p18*$^{-/-}$.*lpr* than in *B6.lpr LNs*, but there was no difference for Tregs. In addition, we now report that p18 deficiency does not affect CD69 expression on T cells (Fig. 4A). Overall, this data suggest that the expansion of DN and B220$^+$ T cells, as well as that of activated and CD4$^+$ Teff cells mapped to both the *Sle2c1.rec1a* and *Sle2c1.rec1d* intervals, but these two intervals were not equivalent. Within *Sle2c1.rec1d*, *Sle2c1.rec1c* provided a significant contribution to T cell activation. In addition, there is some evidence that the

phenotypes of the *Sle2c1.rec1a* interval were not completely accounted for by p18-deficiency, with a potential additional locus within *Sle2c1.rec1a.*

Renal and skin pathology map to the Sle2c1.re1d locus

Proteinuria at 4–6 months of age was negligible (≤ 30 mg/ml) and similar between all congenic lines and B6.*lpr* controls. Differences were however found in renal pathology scores. The renal pathology of 4–6 month old B6.*lpr* mice was limited to a mild mesangial expansion.[12, 14] We found significantly increased GN scores in *Sle2c1.rec1a.lpr*, *Sle2c1.rec1d.lpr* and *Sle2c1.rec1.lpr* as compared to B6.*lpr* mice, and each of these congenic *Sle2c1* recombinant strain presented a different renal pathology (Fig. 5A and B). There was no difference in GN scores between *Sle2c1.rec1a.lpr* and B6.$p18^{-/-}$.lpr mice. Their pathology was characterized by a mesangial expansion with increased cellularity. *Sle2c1.rec1d.lpr* mice presented a significantly more severe phenotype than *Sle2c1.rec1a.lpr* mice, and the type of lesions was qualitatively different with the *Sle2c1.rec1d.lpr* kidneys being characterized by glomerular cell proliferation as well as cellular infiltrates of a mixed population of lymphocytes and monocytes. Finally, GN scores were equivalent between *Sle2c1.rec1.lpr* and *Sle2c1.rec1d.lpr* mice, corresponding to class IV lupus nephritis, and these scores were significantly greater than in *Sle2c1.rec1a.lpr* mice (Fig. 5B). However, only the whole *Sle2c1.rec1* interval conferred a high penetrance of sub-endothelial hyaline glomerular deposits (Fig. 5B), indicating that a predominant role of autoantibodies and immune complexes in these lesions.

We have previously reported that about 20% of *Sle2c1.lpr* mice develop dermatitis but no skin lesions were observed in either B6.$p18^{-/-}$.*lpr* or B6.*lpr* mice.[12, 14] Dermatitis was observed in some of the recombinant mice, particularly in the *Sle2c1rec1d.lpr* strain. The mice typically experienced hair loss, skin ulceration and scab formation on the interscapular and neck regions and the ears (Fig. 6A), as described in B6.*Sle2c1.lpr* mice.[12] The histology assessment of the lesions showed inflammatory cell infiltration, epidermal hyperplasia and ulceration in *Sle2c1.rec1d.lpr* skins (Fig. 6B). B6.*lpr* as well as *Sle2c1.rec1b.lpr* and *Sle2c1.rec1c.lpr* mice never developed dermatitis (Fig. 6C and data not shown), and showed a normal skin architecture and morphology (Fig. 6B). Among the three other strains, *Sle2c1.rec1d.lpr* mice showed the highest incidence of dermatitis (39%, 23/59) which was significantly higher than in either *Sle2c1.rec1.lpr* (12%, 9/85) or *Sle2c1.rec1a.lpr* (5%, 2/38) mice (Fig. 7C), and was even higher than in *Sle2c1.lpr* mice (13/56, $p = 0.034$). The major components of the cellular infiltrates in the skin lesions of *Sle2c1.rec1d.lpr* mice were $CD3^+$ T cells, the majority of which being DN, and $Ly6G^+$ neutrophils (Fig.6D and E). In addition, the *Sle2c1.rec1d.lpr* skin lesions contained smaller but significantly higher amounts of DCs (Fig. 6F), $CD4^+$ and $CD8^+$ T cells as compared with B6.*lpr*.

These results show that the *rec1d* interval contains genetic variation supporting the development of T cell driven autoimmune pathology in both the skin and the kidney. The *rec1a* interval supports only a mild induction of renal pathology in a manner that is consistent with p18-deficiency being the main contributor to the phenotype. There is evidence however of an additional locus in the *Sle2c1.rec1a* interval that, when co-expressed with the other loci, is required for hyaline deposits in addition to the proliferative

GN pathology. This third locus does not seem to be involved in skin pathology, and it may actually be protective.

DISCUSSION

We have previously reported that *Sle2* and *Sle2c1* expression regulates B cell differentiation and homeostasis.[6, 7, 10] In addition, *Sle2c1* greatly enhances the lymphadenopathy and accelerated autoimmune pathology associated with CD95 deficiency.[12] We have showed that p18-deficiency, the genetic variation responsible for the altered B cell homeostasis in *Sle2c1*, was not sufficient to account for the autoimmune phenotypes of *Sle2c1.lpr* mice.[14] The current study used five new recombinant intervals within *Sle2c1* to map these phenotypes and established the existence of three non-redundant loci. One of these loci interacting with CD95 deficiency is located in the middle of the interval and is likely the *Cdkn2c* gene, or a gene closely linked to it. The two other ones, a telomeric interval of about 2 Mb and a larger centromeric interval, each enhance the autoimmune phenotype of the *Cdkn2c*-linked middle locus.

The middle locus corresponding to the overlapping region between *rec1a* and *rec1d* in the middle of the interval exerted the strongest effects on the development of autoimmune pathology, as shown by several phenotypes. First, the *Sle2c1.rec1a.lpr* and *Sle2c1.rec1d.lpr* mice showed a remarkable T cell expansion, reflected by a significant increase in both percentages and absolute numbers in the spleen and LNs as compared to B6.*lpr* controls. This phenotype suggests that the susceptibility gene in the *rec1a/rec1d* overlap affects T cell proliferation. Since T cells were also significantly expanded in B6.$p18^{-/-}$.*lpr* mice, our results are consistent with the combination of p18 and CD95 deficiencies resulting in the preferential proliferation of T cells. We have also detected a marked decrease in the percentage of B cells in *Sle2c1.rec1.lpr*, *Sle2c1.rec1a.lpr* and *Sle2c1.rec1d.lpr* mice. This raises the question why T cells behave differently from B cells in these strains, with the possibility that the increased in absolute B cell numbers is secondary to the T cell expansion. Second, the presence of the rec1a/rec1d overlap was required for all phenotypes, except for the expansion of DN T cells and Teffs in LN for which *Sle2c1.rec1* expression was sufficient. It is well recognized that T cells play a critical role in lupus,[18, 19] The massively expanded T cells, specifically $CD3^+$ $B220^+$ T, DN-T, activated $CD4^+$ T and $CD4^+$ Teff, as well as a striking reduction in percentage of Treg cells in the *Sle2c1.rec.lpr* congenic lines most likely participate in autoimmune pathogenesis, as T cells represent a large fraction of infiltrates in their kidneys,[12] and skin (this report). Finally, significant enhancement of anti-nuclear autoAb production, severe renal and skin pathology required the combination of the *rec1a/rec1d* overlap and the *Sle2c1.rec1c* interval in the *Sle2c1.rec1d.lpr* mice, in which the incidence of inflammatory dermatitis was close to that reported in the MRL-lpr strain, which is a well-established model of spontaneous autoimmune dermatitis.[20] The large number of neutrophils and T cells found in the skin lesions of the *Sle2c1.rec1d.lpr* mice is also reminiscent of the findings in the MRL-lpr mice and in human cutaneous.[21, 22]

These data are consistent with the majority of the *Sle2c1.lpr* autoimmune phenotypes result from interactions between *p18*-deficiency and the *Sle2c1.rec1c* locus, providing additional evidence for the importance of genetic epistasis in lupus.[23] It is possible that other genes

than *p18* contained in the *rec1a/rec1d* overlap are responsible for the *Sle2c1.lpr* autoimmune phenotypes. The *skint* gene family, which consists of eleven members, is located in this region, and *Skint1* regulates epidermal $_{\gamma\delta}$T cell selection,[24, 25] as well as the balance of IFNγ and IL-17 by these cells.[26] The presence of $_{\gamma\delta}$T cells in the skin and renal lesions of *Sle2c1.rec1d.lpr* mice will have to be investigated. The *Sle2c1.rec1c* locus covers ~ 2 Mbp that is gene-rich with 34 known protein-coding genes. We are currently in the process of screening these genes for coding and expression polymorphisms.

Finally, the existence of a susceptibility locus in the *Sle2c1.rec1b* interval is suggested by the reduction in the number of Tregs in the *Sle2c1.rec1b.lpr* LNs and by the more severe renal pathology in *Sle2.rec1.lpr* mice as compared to *Sle2.rec1d.lpr* mice. The absence of proteinuria is most likely due to the fact that these mice have to euthanized due to lymphadenopathy and eventually dermatitis before clinical consequences of renal pathology can develop. Although both strains present a class IV nephritis, the presence of hyaline wire-loop deposits in *Sle2.rec1.lpr* kidneys suggest additional factors favoring the formation and/or deposition of large immune complexes. We have not found any differences in cellular phenotypes between *Sle2.rec1.lpr* and *Sle2.rec1d.lpr* mice, and it is not clear why the presence of the *Sle2c1.rec1b* would exacerbate renal pathology but ameliorate skin pathology. A recent study showed that MyD88 signaling in dendritic cells was critical for dermatitis but not nephritis in MRL/lpr mice,[27] clearly indicating a different mechanism for pathology in the two target organs. *Sle2c1.rec1b* is still a relative large ~ 6 Mbp interval with 43 known protein-coding genes, none of which being an obvious candidate for the reported phenotypes.

In summary, we have shown the existence of two loci within *Sle2c1* that synergize with p18 deficiency to greatly accelerate T-cell mediated autoimmune kidney and skin pathology in CD95 deficient mice. These two loci are not redundant and differentially affect skin and renal pathology. The identification of these genes within the intervals that we have defined will advance our understanding of the complex genetic architecture of lupus susceptibility.

Materials and methods

Mice

The *Sle2c1.lpr* and B6.*p18*$^{-/-}$.*lpr* strains have been previously described.[12, 14] The recombinant congenic intervals *Sle2c1.rec1*, *Sle2c1.rec1a* and *Sle2c1.rec1b*, also previously described,[10] were crossed to homozygosity to B6.*Fas*^{lpr} (B6.*lpr*), which were originally purchased from the Jackson Laboratory. In addition, two new recombinant strains, *Sle2c1.rec1c.lpr* and *Sle2c1.rec1d.lpr*, were produced from *Sle2c1.lpr* mice by repeated backcrossing with B6.*lpr* mice and intercrossing to homozygosity. Both males and females were analyzed at 4–6 months of age. Age- and gender-matched B6.*lpr* mice were used as control. All experiments were conducted according to protocols approved by the Institutional Animal Care and Use Committee of the University of Florida.

The p18 promoter SNP has been previously reported.[13] Two novel polymorphic SNPs, Novel3 (NCBI M37 112653568 C/A)and Novel5 (NCBI M37 113479088 C/T) were identified through sequencing of captured target genomic fragments performed at the UF

Interdisciplinary Center for Biotechnology Research. Briefly, based on the NCBIM37 mouse genome sequence, probe design and capture array manufacture were performed with Agilent Technologies reagents to target the chr4:108560000-115000000 region. Genomic DNA was prepared from a *Sle2c1.rec1d.lpr* mouse. 100-800bp DNA fragments were made by shearing and then hybridized with the capture array. After unbound DNA fragments were washed off, the captured DNA fragments were eluted and sequenced by paired-end (2×100) NGS protocol on Illumina HiSeq2000. The raw sequence data was mapped to the reference B6 genome (NCBIM37) to identify SNPs. Fine mapping of the recombinants was performed by PCR for microsatellites markers and direct Sanger sequencing for SNPs.

Autoantibody measurements

Anti-dsDNA and anti-chromatin IgG were measured by ELISA as previously described.[28] Briefly, mBSA-precoated plates were coated overnight with 50 *m*g/ml dsDNA; with the addition of 10 *m*g/ml of histone H1, H2A, H2B, H3 and H4 overnight for anti-chromatin IgG measurement. 1:100 diluted test sera were added to the plates and bound autoantibodies were detected using alkaline phosphatase-conjugated goat anti-mouse IgG and pNPP substrate. Raw optical densities were converted to units per milliliter, using a standard curve derived from pooled B6.*Sle1.Sle2.Sle3* sera, arbitrarily setting the reactivity of a 1:100 dilution of this serum to 100 U/ml.

Flow cytometry

Cell subset distribution and activation in the spleen and LN were determined by flow cytometry as previously described.[12] In brief, single-cell suspensions were prepared by lysing red blood cells with 0.83% NH_4Cl. Afterwards, cells were blocked with saturating amounts of anti-CD16/CD32 (2.4G2) and then stained with fluorochrome-conjugated antibodies: CD3e (145-2C11), CD4 (RM4-5), CD8a (53–6.7), CD19 (1D3), CD44(1M7), CD69(H1.2F3), B220 (RA3-6B2). Intracellular staining for FoxP3 (FJK-16s) was performed after fixation/permeabilization of cells. All antibodies were purchased from BD PharMingen or eBioscience. At least 30,000events were acquired per sample using a FACSCalibur cytometer (BD Biosciences).

Kidney and skin pathology

Proteinuria was determined with Albustix strips (Bayer). Kidneys from 4–5 month old mice were fixed and stained with hematoxylin and eosin (H&E) and periodic acid Schiff (PAS). Renal lesions were scored in a blinded manner as previously described.[12] Briefly glomerular lesions were classified as negative (N), mesangial matrix (PAS^+ Mm) or mesangial cellularity (Mc) expansion or proliferative glomerulonephritis (glomerular hypercellularity, P). Extent of involvement was graded on a 1-4 scale in both M and P categories. In addition, the presence of heavy hyaline PAS^+ deposits was noted.

The incidence of dermatitis was recorded during daily checks. Formalin-fixed skin specimens were embedded in paraffin and sections were stained H&E. Quantitative analysis of cellular infiltrates in skin was conducted as described.[29] Briefly, 1 cm^2 of skin was excised from the dorsal neck of *Sle2c1.rec1d.lpr* mice with or without skin lesions and from B6.*lpr* mice (all without skin lesions). The dermis was separated mechanically from the

epidermis and digested with 0.28 U/ml Liberase 3 (Roche) for 20 min at 37°C, passed through a 70-μm filter and washed in serum-free RPMI. The resulting cells were stained with fluorochrome-conjugated antibodies against the following lineage markers CD3e (145-2C11), CD4 (RM4-5), CD8a (53–6.7), CD19 (1D3), CD11b(M1/70), CD11c(HL3), CD45(30-F11), F4/80(BM8)and Ly6G (1A8). All samples were analyzed with a FACSCallibur at high speed for one minute in order to get the relative cell number per sample.

Statistical analysis

Data was analyzed with GraphPad Prism 5.0 software with the statistical tests indicated in the text. Non-parametric tests were used when data were not distributed normally. Multiple comparison tests were performed using either Bonferonni or Dunns' tests. Means, SEM, and the levels of statistical significance are shown in the figures.

Acknowledgements

This work was supported by National Institutes of Health grants K01-AR-056725-01 (ZX) and R01-AI-068965 (L.M.). We thank the members of the Morel lab for stimulating discussions, Leilani Zeumer for technical help as well as Nathalie Kanda for outstanding animal care.

Abbreviations used in this paper

SLE	Systemic lupus erythematosus
autoAb	autoantibodies
B6	C57BL/6
GN	glomerulonephritis
SNP	single nucleotide polymorphism
LN	lymph node
DN	$CD4^-$ $CD8^-$ double negative
Teff	$CD4^+$ $CD44^+$ effector T cells
Treg	$CD4^+$ $FoxP3^+$ regulatory T cells
H&E	hemotoxylin and eosin
PAS	periodic acid Schiff.

References

1. Tsokos GC. Systemic lupus erythematosus. N Engl J Med. 2011; 365:2110–2121. [PubMed: 22129255]
2. Vaughn SE, Kottyan LC, Munroe ME, Harley JB. Genetic susceptibility to lupus: the biological basis of genetic risk found in B cell signaling pathways. J Leukoc Biol. 2012; 92:577–591. [PubMed: 22753952]
3. Morel L. Genetics of SLE: evidence from mouse models. Nat Rev Rheumatol. 2010; 6:348–357. [PubMed: 20440287]

4. Morel L, Rudofsky UH, Longmate JA, Schiffenbauer J, Wakeland EK. Polygenic control of susceptibility to murine systemic lupus erythematosus. Immunity. 1994; 1:219–229. [PubMed: 7889410]
5. Morel L, Croker BP, Blenman KR, Mohan C, Huang G, Gilkeson G, et al. Genetic reconstitution of systemic lupus erythematosus immunopathology with polycongenic murine strains. Proc Natl Acad Sci USA. 2000; 97:6670–6675. [PubMed: 10841565]
6. Mohan C, Morel L, Yang P, Wakeland EK. Genetic dissection of systemic lupus erythematosus pathogenesis - Sle2 on murine chromosome 4 leads to B cell hyperactivity. J Immunol. 1997; 159:454–465. [PubMed: 9200486]
7. Xu Z, Butfiloski EJ, Sobel ES, Morel L. Mechanisms of peritoneal B-1a cells accumulation induced by murine lupus susceptibility locus Sle2. J Immunol. 2004; 173:6050–6058. [PubMed: 15528340]
8. Liu Y, Li L, Kumar KR, Xie C, Lightfoot S, Zhou XJ, et al. Lupus susceptibility genes may breach tolerance to DNA by impairing receptor editing of nuclear antigen-reactive B cells. J Immunol. 2007; 179:1340–1352. [PubMed: 17617627]
9. Zeumer L, Sang A, Niu H, Morel L. Murine lupus susceptibility locus Sle2 activates DNAreactive B cells through two sub-loci with distinct phenotypes. Genes Immun. 2011; 12:199–207. [PubMed: 21270826]
10. Xu Z, Duan B, Croker BP, Wakeland EK, Morel L. Genetic dissection of the murine lupus susceptibility locus Sle2 : contributions to increased peritoneal B-1a cells and lupus nephritis map to different loci. J Immunol. 2005; 175:936–943. [PubMed: 16002692]
11. Xu Z, Vallurupalli A, Fuhrman C, Ostrov D, Morel L. An NZB-derived locus suppresses chronic graft versus host disease and autoantibody production through non-lymphoid bone marrow derived cells. J Immunol. 2011; 186:4130–4139. [PubMed: 21335485]
12. Xu Z, Cuda CM, Croker BP, Morel L. The NZM2410-derived lupus susceptibility locus Sle2c1 increases TH17 polarization and induces nephritis in Fas-deficient mice. Arthritis Rheum. 2011; 63:764–774. [PubMed: 21360506]
13. Potula HH, Morel L. Genetic variation at an YY-1 response site regulates the transcription of cyclin-dependent kinase inhibitor $p18^{INK4C}$ transcript in lupus-prone mice. J Immunol. 2012; 188:4992–5002. [PubMed: 22504641]
14. Potula HH, Xu Z, Zeumer L, Sang A, Croker BP, Morel L. Cyclin-dependent kinase inhibitor *Cdkn2c* deficiency promotes B1a cell expansion and autoimmunity in a mouse model of lupus. J Immunol. 2012; 189:2931–2940. [PubMed: 22896639]
15. Shi X, Xie C, Kreska D, Richardson JA, Mohan C. Genetic dissection of SLE: SLE1 and FAS impact alternate pathways leading to lymphoproliferative autoimmunity. J Exp Med. 2002; 196:281–292. [PubMed: 12163557]
16. Watanabe-Fukunaga R, Brannan CI, Copeland NG, Jenkins NA, Nagata S. Lymphoproliferation disorder in mice explained by defects in Fas antigen that mediates apoptosis. Nature. 1992; 356:314–317. [PubMed: 1372394]
17. Budd RC, Van Houten N, Clements J, Mixter PF. Parallels in T lymphocyte development between lpr and normal mice. Semin Immunol. 1994; 6:43–48. [PubMed: 8167306]
18. Shin MS, Lee N, Kang I. Effector T-cell subsets in systemic lupus erythematosus: update focusing on Th17 cells. Curr Opin Rheumatol. 2011; 23:444–448. [PubMed: 21720245]
19. Moulton VR, Tsokos GC. Abnormalities of T cell signaling in systemic lupus erythematosus. Arthritis Res Ther. 2011; 13:207. [PubMed: 21457530]
20. Furukawa F, Yoshimasu T. Animal models of spontaneous and drug-induced cutaneous lupus erythematosus. Autoimm Rev. 2005; 4:345–350.
21. Ghoreishi M, Dutz JP. Murine models of cutaneous involvement in lupus erythematosus. Autoimmun Rev. 2009; 8:484–487. [PubMed: 19239927]
22. Yang JQ, Chun T, Liu H, Hong S, Bui H, Van Kaer L, et al. CD1d deficiency exacerbates inflammatory dermatitis in MRL-lpr/lpr mice. Eur J Immunol. 2004; 34:1723–1732. [PubMed: 15162443]
23. Rose AM, Bell LC. Epistasis and immunity: the role of genetic interactions in autoimmune diseases. Immunol. 2012; 137:131–138.

24. Boyden LM, Lewis JM, Barbee SD, Bas A, Girardi M, Hayday AC, et al. Skint1, the prototype of a newly identified immunoglobulin superfamily gene cluster, positively selects epidermal [gamma] [delta] T cells. Nat Genet. 2008; 40:656–662. [PubMed: 18408721]

25. Barbee SD, Woodward MJ, Turchinovich G, Mention JJ, Lewis JM, Boyden LM, et al. Skint-1 is a highly specific, unique selecting component for epidermal T cells. Proc Natl Acad Sci USA. 2011; 108:3330–3335. [PubMed: 21300860]

26. Turchinovich G, Hayday AC. Skint-1 identifies a common molecular mechanism for the development of interferon-gamma-secreting versus interleukin-17-secreting gammadelta T cells. Immunity. 2011; 35:59–68. [PubMed: 21737317]

27. Teichmann LL, Schenten D, Medzhitov R, Kashgarian M, Shlomchik MJ. Signals via the adaptor MyD88 in B cells and DCs make distinct and synergistic contributions to immune activation and tissue damage in lupus. Immunity. 2013; 38:528–540. [PubMed: 23499488]

28. Mohan C, Alas E, Morel L, Yang P, Wakeland EK. Genetic dissection of SLE pathogenesis - Sle1 on murine chromosome 1 leads to a selective loss of tolerance to H2A/H2B/DNA subnucleosomes. J Clin Invest. 1998; 101:1362–1372. [PubMed: 9502778]

29. Guiducci C, Tripodo C, Gong M, Sangaletti S, Colombo MP, Coffman RL, et al. Autoimmune skin inflammation is dependent on plasmacytoid dendritic cell activation by nucleic acids via TLR7 and TLR9. J Exp Med. 2010; 207:2931–2942. [PubMed: 21115693]

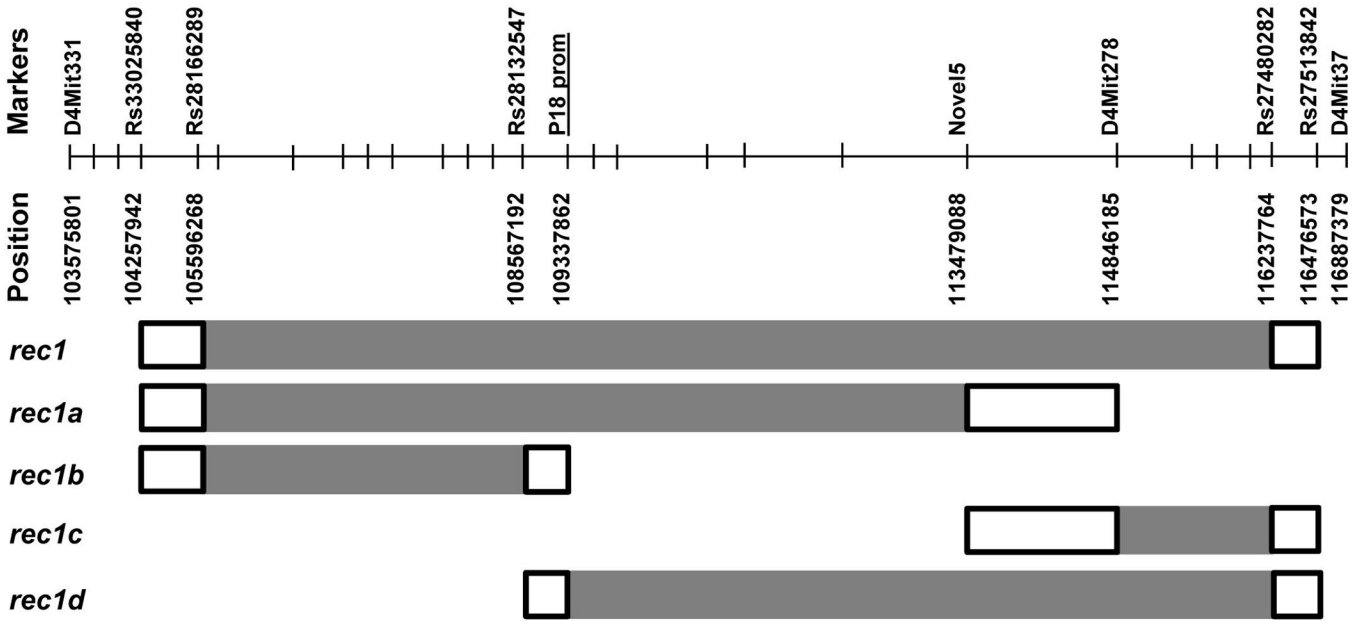

Figure 1. Physical map of the *Sle2c1.rec1* locus and its derived sub-loci

The grey rectangles show the NZB homozygous intervals corresponding to *Sle21c1.rec1* (*rec1*) and its derived recombinants, *rec1a*, *rec1b*, *rec1c* and *rec1d* on the B6 genetic background. The white rectangles indicate the areas of recombination between the two genomes. The fine mapping and boundaries of these intervals were determined using a combination of markers that are polymorphic between the NZB and B6 genomes, including microsatellites as well as SNPs obtained from public databases and our own genomic sequencing, such Novel5. For clarity purposes, only the terminal markers are displayed on the top panel. The entire list of makers used is provided in Table 1. The lower panel reveals the positions of the markers according to Ensembl NCBI m37.

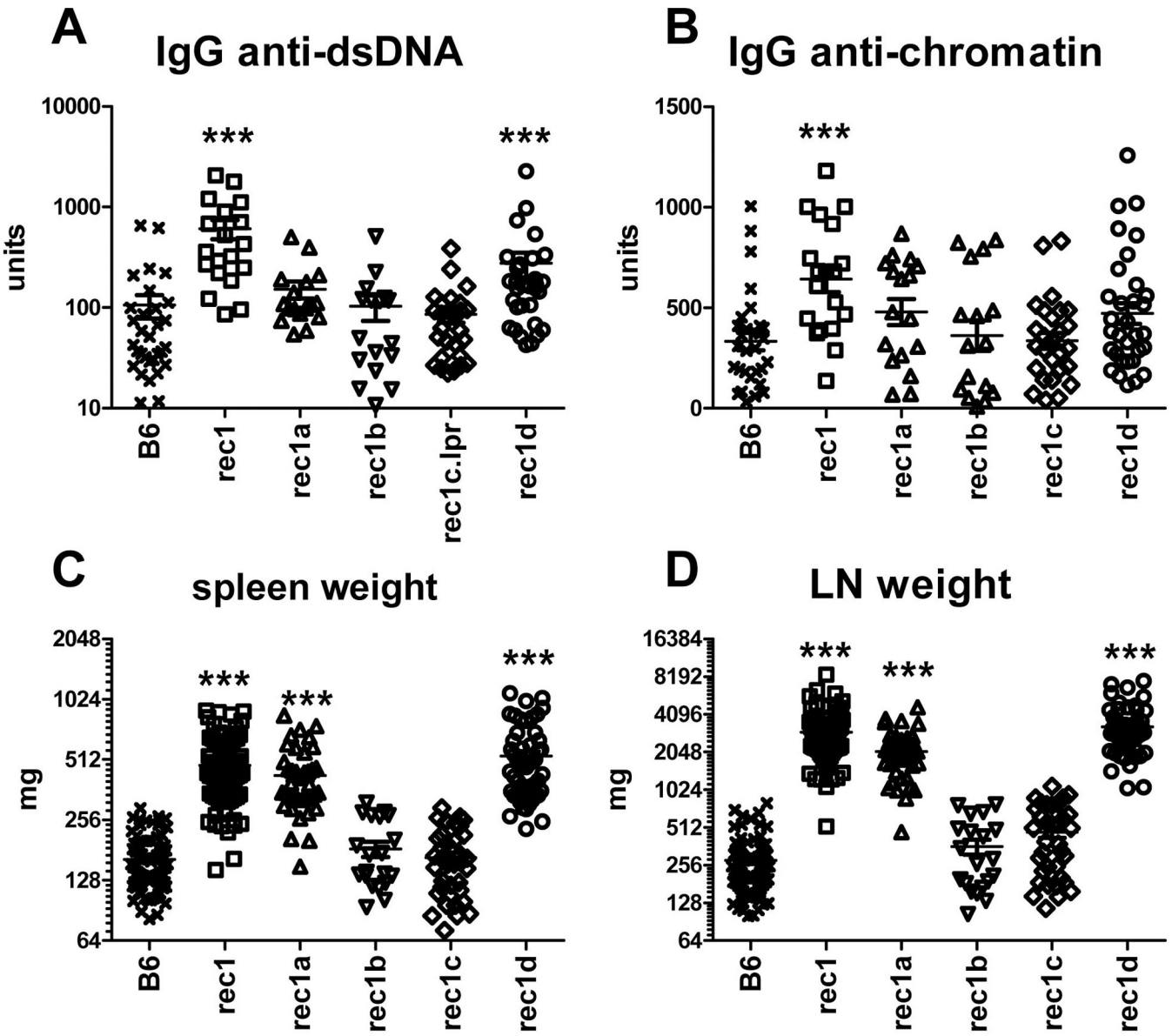

Figure 2. ***Sle2c1.rec1.lpr*** **antinuclear autoantibody production and lymphoid expansion map to** ***Sle1c1.rec1d*** **and** ***Sle1c1.rec1a***

Serum levels of anti-dsDNA IgG (**A**) and anti-chromatin IgG (**B**). Spleen (**C**) and pooled lymph nodes (**D**) weight. Results are expressed as units and are relative to a standard curve derived from a serum pool of aged B6.*Sle1*.*Sle2*.*Sle3* mice. Statistical analysis was performed using Dunn's multiple comparison tests with B6.*lpr* values. ***$p < 0.001$.

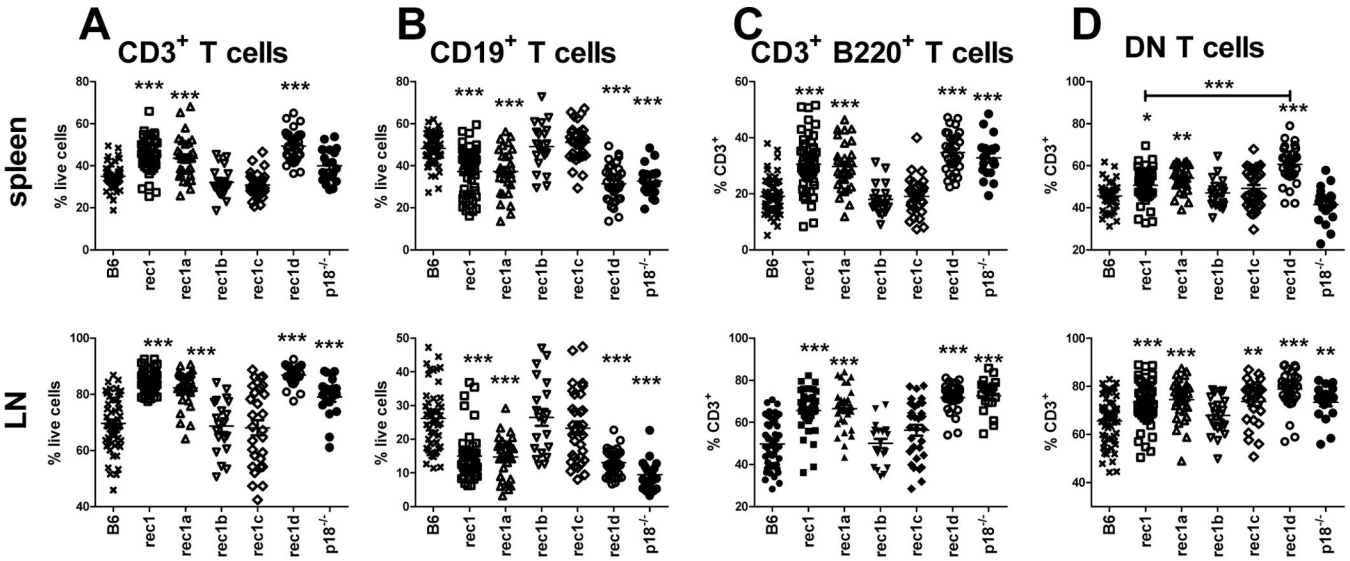

Figure 3. *Sle2c1.rec1.lpr* T cell expansion maps to two loci

Percentages of $CD3^+$ T cells (**A**), $CD19^+$ B cells (**B**), $CD3^+$ $B220^+$ T cells (**C**) and DN T cells (**D**) in spleens (top row) and LNs (bottom row). Statistical analysis was performed using Dunn's multiple comparison tests with B6.*lpr* values. In addition, the comparison between *rec1* and *rec1d* are shown in **D**, ***$p < 0.001$.

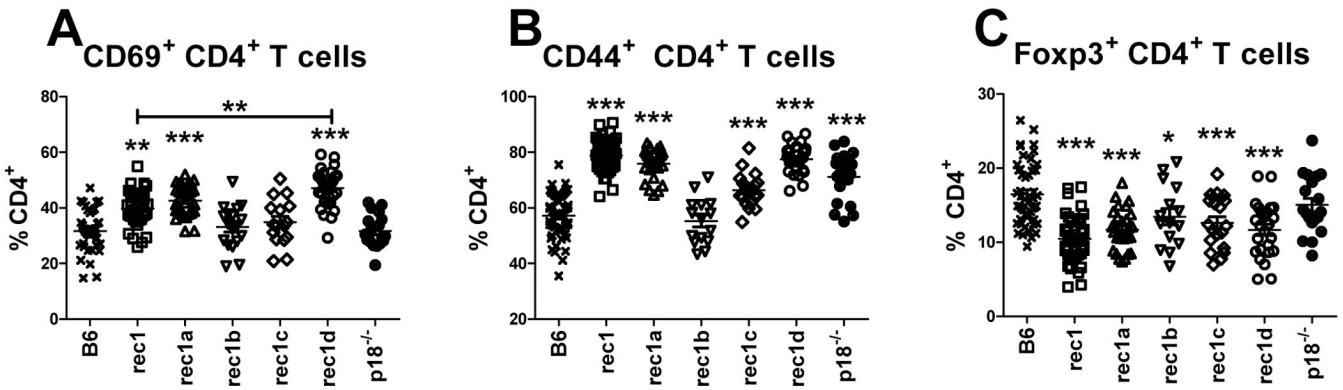

Figure 4. ***Sle2c1.rec1.lpr*** **T cell effector phenotypes map to two loci**

Percentage of $CD69^+$ (**A**), $CD44^+$ (**B**) and $FoxP3^+$ (**C**) $CD4^+$ T cells in the LNs of the indicated strains. Statistical analysis was performed using Dunn's multiple comparison tests with B6.*lpr* values. In addition, the comparison between *rec1* and *rec1d* are shown in **A**, $*p < 0.05$; $**p < 0.01$; $***p < 0.001$.

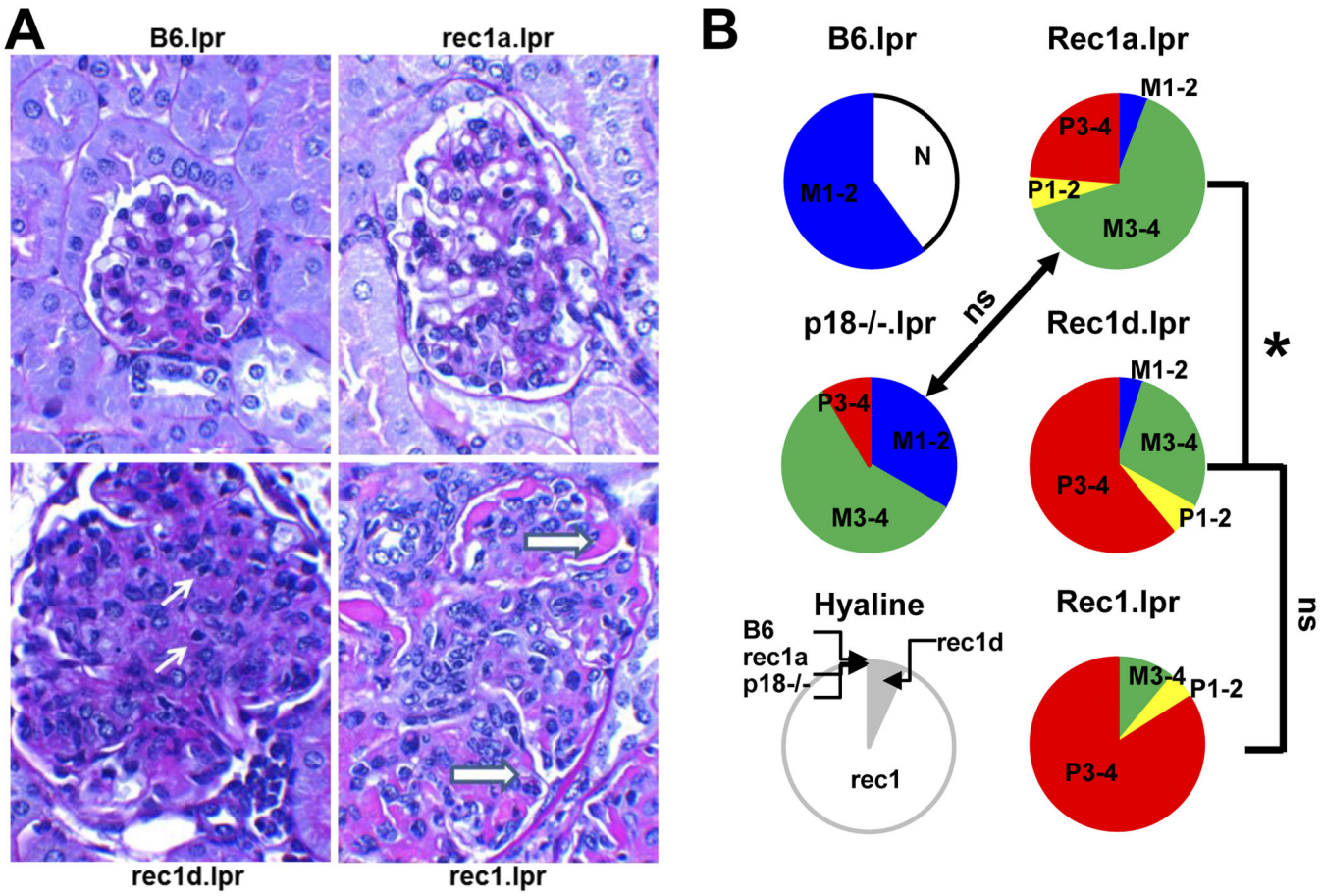

Figure 5. p18 deficiency and the *rec1d* locus contribute to renal pathology in the *Sle2c1.rec1.lpr* mice

A. Representative PAS-stained kidney sections from B6.*lpr*, *Sle2c1.rec1a.lpr*, *Sle2c1.rec1d.lpr* and *Sle2c1.rec1.lpr* mice. All images in this figure were photographed at the same magnification (100× oil immersion objective) and maintained through preparation. Therefore the sizes of the glomeruli are representative and are a marker of inflammation. B6.*lpr* (score Mm2) shows macula densa at 6 o'clock. There is minimal deviation from normal with mild increase in mesangial matrix in a minority of glomeruli. *Sle2c1.rec1a.lpr* (score Mc4) shows afferent arteriole at 4–5 o'clock, with further increased mesangium and mesangial hypercellularity in a larger percentage of glomeruli. Capillary walls and lumens are generally preserved. *Sle2c1.rec1d.lpr* (score P global 4) shows stalk region at 4 – 5 o'clock. There is additional hypercellularity with involvement of the capillary walls and lumens. Small lymphocytes (white arrows) are prominent. *Sle1c2.rec1.lpr* (score Pg4) shows glomerular vascular pole at 10 o'clock. There are many activated cells with large, open, vesicular nuclei. Capillaries are compromised by cells and contain large sub-endothelial immune complex hyaline deposits (wire loops, arrow heads). **B**. Quantitation of renal pathology scores from at least 15 mice per strain. The pie charts show the distribution (percentages) of renal pathology scores grouped as N (white): negative; M1-2 (blue): mild mesangial expansion; M3-4 (green): severe mesangial expansion; P1-2 (yellow): mild proliferative; P3-4 (red): severe proliferative. The black and white "Hyaline" pie chart

shows the percentage of mice presenting with heavy glomerular hyaline deposits for each strain. No incidence of this phenotype was observed in B6.*lpr*, *Sle1c1.rec1a.lpr* and B6.$p18^{-/-}$.*lpr* mice. Statistical comparisons between strains were performed with two-tailed Fisher exact tests comparing grouped mild GN scores (M1-2 + M3-4 + P1-2) to severe GN scores (P3-4). *$p < 0.05$, ns: not significant.

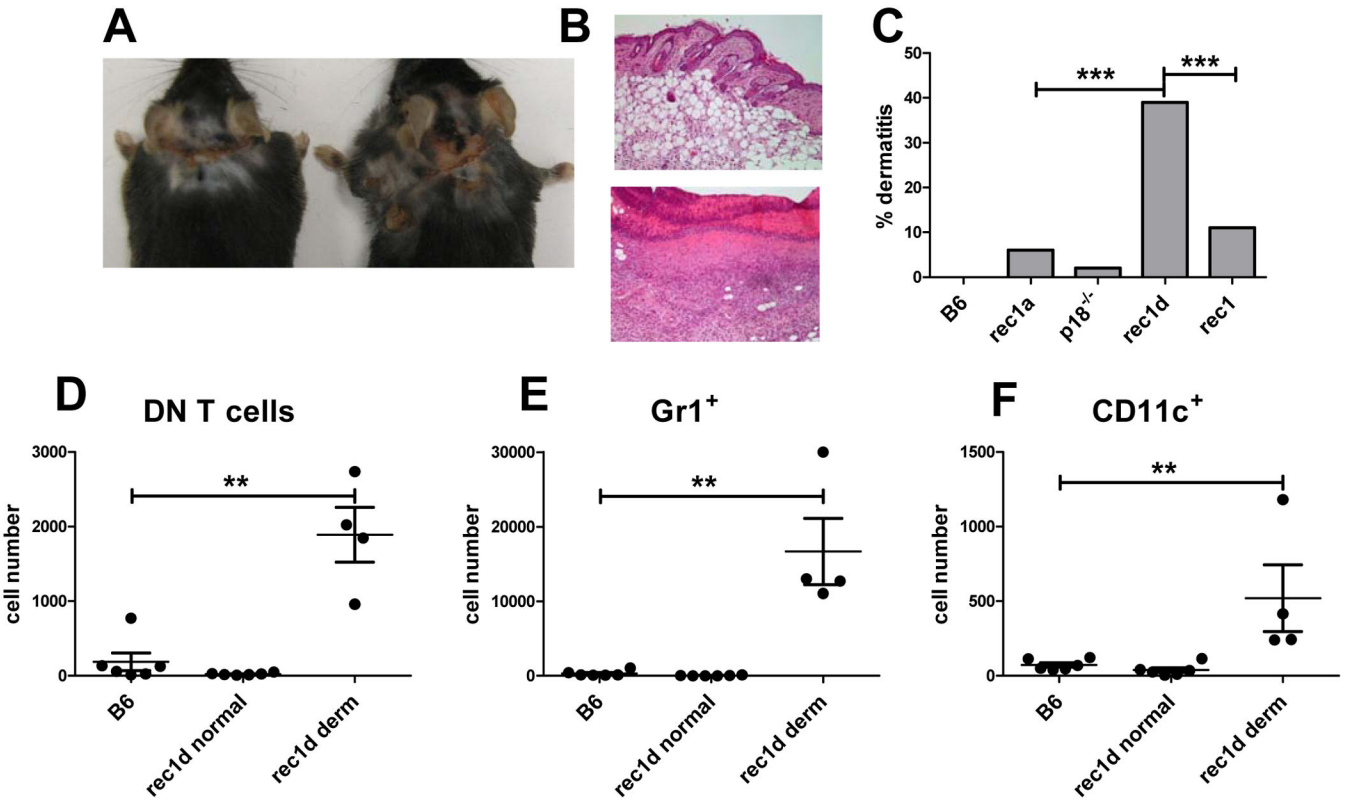

Figure 6. The *rec1d* locus contributes to skin pathology

A. Representative *Sle1c1.rec1d.lpr* mice showing a typical interscapular dermatitis. **B**. Representative H&E stained interscapular skin sections from an unaffected B6.lpr mouse (top) and from a lesion in a *Sle1c1.rec1d.lpr* mouse. **C**. Frequency of dermatitis B6.lpr: N = 50; *Sle1c1.rec1a.lpr:* N =38; B6.$p18^{-/-}$*.lpr:* N = 50; *Sle1c1.rec1d.lpr*: N = 59; and *Sle2c1.rec1.lpr*: N = 85. Absolute numbers of DN T cells (**D**), $Gr1^+$ granulocytes (**E**) and $CD11c^+$ dendritic cells (**F**) collected from 1 cm^2 of interscapular skin from B6.*lpr*, unaffected (normal) or affected (derm) *Sle1c1.rec1d.lpr* mice. Statistical comparisons were performed with two-tailed Mann-Whitney tests; $^{**}p < 0.01$.

Table 1

Fine mapping to the Sle2c1.rec1 loci

SNPs & markers	Position[1]	rec1	rec1a	rec1b	rec1c	rec1d
D4Mit331	103575801	B[2]	B	B	B	B
rs32095460	103755131	B	B	B	B	B
rs28154332	103913531	B	B	B	B	B
rs33025840	104257942	B	B	B	B	B
rs28166289	105596268	N[3]	N	N	B	B
rs3664701	105891733	N	N	N	B	B
rs28327171	106685675	N	N	N	B	B
rs32014282	107076284	N	N	N	B	B
rs28162653	107669976	N	N	N	B	B
rs33011000	107720590	N	N	N	B	B
rs28150412	108531685	N	N	N	B	B
rs32270804	108549143	N	N	N	B	B
rs28132605	108551173	N	N	N	B	B
rs28132547	108567192	N	N	N	B	B
p18 promoter	109337862	N	N	B	B	N
rs13477908	109908297	N	N	B	B	N
rs32194443	111068240	N	N	B	B	N
rs47071801	111648032	N	N	B	B	N
novel3	112653568	N	N	B	B	N
novel5	113479088	N	N	B	B	N
D4Mit278	114846185	N	B	B	N	N
rs27495341	115561566	N	B	B	N	N
rs32080914	115575513	N	B	B	N	N
rs4224727	115975049	N	B	B	N	N
rs27480282	116237764	N	B	B	N	N
rs27513842	116476573	B	B	B	B	B
D4Mit37	116887379	B	B	B	B	B

[1] NCBIM37 release

[2] B6 allele

[3] NZB allele